Habitat International 58 (2016) 75–88

Contents lists available at ScienceDirect

Habitat International

journal homepage: www.elsevier.com/locate/habitatint

Spatiotemporal patterns of urban change and associated environmental impacts in five Saudi Arabian cities: A case study using remote sensing data

Abdullah F. Alqurashi [a, b, *], Lalit Kumar [a]

[a] School of Environmental and Rural Science, University of New England, Armidale, NSW, 2351, Australia
[b] Department of Geography, Umm Al-Qura University, Makkah, 21955, Saudi Arabia

ARTICLE INFO

Article history:
Received 1 December 2015
Received in revised form
26 September 2016
Accepted 3 October 2016
Available online 12 October 2016

Keywords:
Urbanization
Change detection
Landsat images
OBIA
Environmental impacts
Saudi Arabia

ABSTRACT

Urban growth is a serious threat and challenge worldwide due to its role in altering ecosystem processes and contributing to negative environmental impacts. The natural environment of Saudi Arabia has been affected by the increased pace of urban and economic development, which has been supported by large oil revenues in recent years. Measuring the spatiotemporal patterns of urban growth is important to better understand the qualitative and quantitative impacts of urban spatial distribution over periods of time. Optical remote sensing can be a reliable data source that provides valuable information regarding the spatial and temporal distributions of urban growth. This research used two sets of Landsat images from 1985 and 2014 to map and monitor the spatial distribution of the urban extent among five Saudi Arabian cities: Riyadh, Jeddah, Makkah, Al-Taif and Eastern Area. A decision tree classifier was applied using object-based image analysis (OBIA) to analyze urban land cover in the five cities. The accuracy assessment of the urban change detection maps indicated a high overall accuracy and Kappa coefficient. The results of this research show a high rate of urbanization and complex dynamics across the five cites. The significant changes were the result of a rapid increase in land development, exhibiting complex patterns in the urbanization process across the five cities. The government's policy and increased oil revenues significantly contributed to increasing the urban cover in the five selected cities.

1. Introduction

1.1. Background

Rapid urbanization is becoming a serious threat and challenge worldwide (Reilly, O'Mara, & Seto, 2009; Wentz, Nelson, Rahman, Stefanov, & Roy, 2008). More than 54% of the global population lives in cities (Seto, 2009; Taubenböck, Wiesner, et al., 2014; Taubenböck, Esch, et al., 2014; Rahman, Aggarwal, Netzband, & Fazal, 2011), which causes a number of associated environmental and health problems (Weng, 2014, pp. 1–12). Urbanization significantly influences local and global earth ecosystems and the services they provide to humans and other life on earth (Alberti, 2005). Ecosystems have been and are currently being altered by human population growth and related developments on a global scale (Giri, 2012; Ramankutty & Foley, 1998; Vitousek, Mooney, Lubchenco, & Melillo, 1997). Thus, urbanization has significant impacts on a number of environmental aspects, including soil loss, topographical changes, emission of pollutants, climate change, surface resources and natural resources. In addition, other non-environmental impacts include socioeconomic and political factors as well as related opportunity and risk (Grimmond, 2007; Martin, 2009; Weng, 2014, pp. 1–12).

Development policy plays an important role in the expansion of urban cover, more than the natural development, in terms of building new structures and increasing transportation and recreation areas (Bobylev, 2009). In addition government support, such as providing loans to public and private sectors, contributes significantly in the expansion of cities. In developing countries, long term urban planning generally does not consider sustainable development and also ecological principles are not taken into account. Thus, the implications of this growth are always massive and a

* Corresponding author. Ecosystem Management, School of Environmental and Rural Science, University of New England, Armidale, NSW, 2351, Australia.
E-mail addresses: aalquras@myune.edu.au (A.F. Alqurashi), lkumar@une.edu.au (L. Kumar).

http://dx.doi.org/10.1016/j.habitatint.2016.10.001
0197-3975/

cause of a number of ecological and health problems as well as a weakness in the cities infrastructure. Understanding past and present urban change at both local and global scales is necessary to address potential future development to avoid negative consequences.

The measurement of urban expansion is important for better understanding how, when and where it occurs (Jia & Jiang, 2010). However, measuring the expansion of urban growth is often a difficult and time consuming task due to its complex dynamics (Taubenböck et al., 2012). Some studies have used population data, land use and road network maps to measure urban growth (Fulton, Pendall, Nguyen, & Harrison, 2001; Pendall, 1999; Torrens, 2008). However, the spatial distribution and dimension of the extent of urbanization is difficult to extract accurately from such data. Additionally, there are time periods when such data were not gathered and, where it has been gathered, public accessibility is often denied (Masek, Lindsay, & Goward, 2000), particularly in developing countries. Data used to measure the spatial and temporal distribution of urban expansion needs to be more accurate and reliable.

Optical remote sensing data, including that with a coarse spatial resolution of 250–1000 m (e.g., MODIS), medium spatial resolution of 30–60 m (e.g., Landsat) and high spatial resolution of 0.5–10 m (e.g., IKONOS, QuickBird, WorldView), can be effectively used to measure and map spatial and temporal land cover changes, including urban expansion. Several studies have monitored the urban extent using such data, including at the coarse spatial resolution (Mertes, Schneider, Sulla-Menashe, Tatem, & Tan, 2014; Schneider, Friedl, & Potere, 2010), medium spatial resolution (Bagan & Yamagata, 2012; Jat, Garg, & Khare, 2008) and high spatial resolution scales (Lu, Hetrick, Moran, & Li, 2010; Small, 2003; Sugg, Finke, Goodrich, Moran, & Yool, 2014). However, long-term change detection costs and small-scale coverage areas limit the use of high resolution data. While coarse resolution data are useful for detecting changes over large areas (countries and continents), a large amount of image calibration is necessary, which is very labor-intensive. Therefore, medium spatial resolution (e.g. Landsat) images are more reliable and cost-effective for long term change detection of urban expansions.

1.2. Saudi Arabian development

Saudi Arabia has developed rapidly over the last 30 years. Growth began when the government began implementing an intense program of development, which was financed by massive oil revenues (Alqurashi & Kumar, 2014; Mubarak, 2004). These revenues were extensively used to enhance development and to support both the public and private sectors by providing no-interest loans (Al-Hathloul & Mughal, 2004; Gamboa, 2008). This led to uncontrolled growth across the country. Like other developing countries, controlling urban sprawl and understanding its negative consequences is difficult, particularly due to a shortage of information regarding the actual distribution and spatial effects of urban cover in Saudi Arabia. Urban growth and its areal distributions are essential data, which are required for a wide range of environmental and socioeconomic applications in rapidly developing areas, such as Saudi Arabia. With fast and dynamic urbanization, there is an urgent need for automatic identification methods, which can be used to update urban cover information to understand the dynamics of spatial and temporal distribution as well as for strategies for future development (Li, Zhou, et al., 2013). Previous research in Saudi Arabia used a single index indicator that was based on population data or existing land use data to measure the distribution of urban cover (e.g., Al-Hathloul & Mughal, 2004; Aljoufie, 2014; Aljoufie, Zuidgeest, Brussel, & van Maarseveen, 2013). However, these types of data cannot provide accurate information for the spatiotemporal measurement of urban expansion.

Remote sensing has been utilized for individual Saudi Arabian cities in the past. For example, Al-Ghamdi and Al-Naggar (2002) visually monitored urban growth in Makkah between 1987 and 2000 using a set of different satellite images. Al-Ghamdi, Mirza, Elzahrany, and Dawod (2012) developed a 4D GIS analysis for monitoring and quantifying urban growth of Makkah between 1990 and 2010. In addition, Alqurashi and Kumar (2014) detected land cover changes and urban expansion in Makkah and Al-Taif using Landsat images between 1986 and 2013. Similarly, Rahman (2016) utilized Landsat images to detect urban land use changes in eastern coastal city of Al-Khobar, Eastern Area between 1990 and 2013. However, a comparative study of the spatial measurement of urban growth for different landscape has not been addressed for long-term change detection in Saudi Arabia.

This research will discuss the role of the country's growing economy on the expansion of urban areas in five Saudi Arabian cities. It seeks to answer the questions of how much the government plans contributed to the rapid development in Saudi Arabian cities and what policies have been implemented over the last 30 years. To answer these questions, we use remote sensing data and techniques to quantify the spatial distribution of urban growth in five Saudi Arabian cities, including, Riyadh, Jeddah, Makkah, Al-Taif and Eastern Area, by analyzing multi-temporal Landsat data of 1985 and 2014. Second, we analyze the causes of urban growth in the five cities in terms of increased oil revenues and government policies. Finally, we discuss the effects of rapid growth in the arid environment of Saudi Arabia and the associated risks to natural resources.

2. Study area

The selected study areas include five cities in Saudi Arabia: Riyadh, Jeddah, Makkah, Al-Taif and Eastern Area (Fig. 1). These cities are considered to be the most urbanized and populated in the country, with Riyadh being the capital and largest city. It is situated in the central part of Saudi Arabia on the large Najd plateau and, according to 2013 census statistics, has a population of 6,079,295. This includes the Al-Kharj Governorate. Jeddah is the largest sea port on the Red Sea coast, a major urban center of western Saudi Arabia and an important commercial hub nationally. With a population of 3,865,873, according to the above census, Jeddah is the largest city in the Makkah Region and second largest in the country. Makkah is the holy place of the Muslim community and is located in the central part of the region, approximately 70 km inland from Jeddah. In 2013, it had a population of 1,867,886. Al-Taif, considered to be the most important tourist city of Saudi Arabia, is the fourth study area in our analysis and is located in the south-eastern part of the Makkah region. It has a population of 1,083,693. Eastern Area is located in eastern Saudi Arabia on the Arabian Gulf and is home to most of Saudi Arabia's oil production. Eastern Area includes 11 towns and governorates spread across the region. Only the most populated five towns, which are Dammam, Al-Khobar, Al-Qatif, RasTanura and Al-Jubail, are considered in this study. The population of these towns totaled 2,713,583 in 2013.

3. Data and methods

3.1. Data and pre-processing

Data used in this study comprised 12 Landsat Thematic Mapper (TM), Operational Land Imager (OLI) images for five cities across Saudi Arabia (Table 1). All 12 images were obtained from the USGS Global Visualization (GloVis) site. As Level 1 products all of the

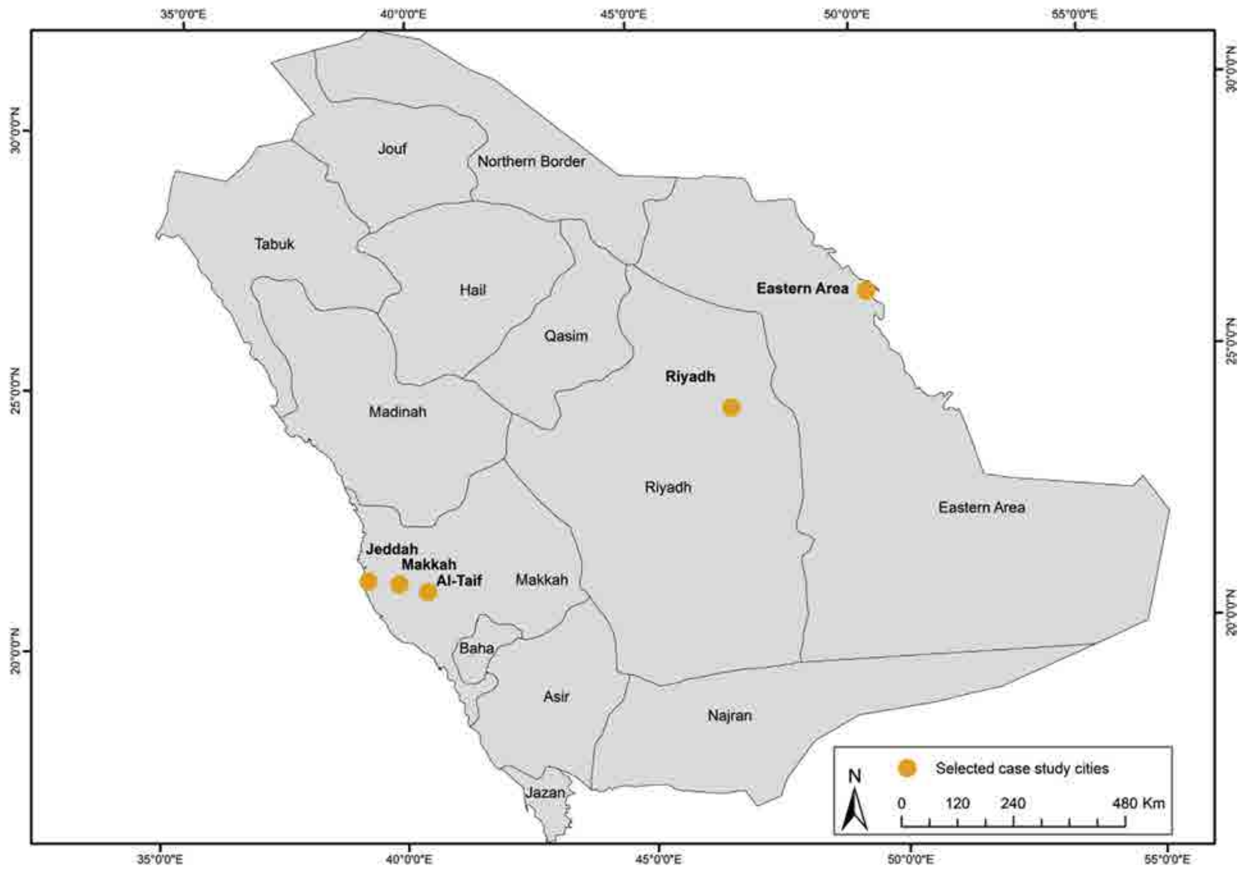

Fig. 1. Spatial distribution of the selected five cities in Saudi Arabia.

images were already geometrically corrected and rectified to UTM zone 37 for Jeddah, Makkah and Al-Taif; zone 38 for Riyadh; and zone 39 for Eastern Area. However, there was a shift in the eastern region, including image path 164 and row 42 of the TM image and image path 165 and row 43 of the Riyadh image. Both images were geo-referenced using OLI images in the same path and row, using the build edges feature to add 20 control points. Mosaic processing was applied to merge two path and row images for Riyadh and Eastern Area to cover the urban footprint. Image subsets were extracted for the five cities, including all of the urban boundaries. Subsets of the selected areas of the Makkah and Al-Taif images did not include the cloud cover in the images. The goal of this paper was to detect the changes in urbanization. Therefore, the hourly time differences between images one and two were not considered, only the sampling dates.

Table 1
Landsat images information used in this study.

No	Path	Row	Sensor	Date	Cloud cover (%)	Covered area
1	164	41	TM	4-Apr-85	1	Eastern Area
2			OLI	2-Aug-14	0	
3	164	42	TM	4-Apr-85	0	
4			OLI	2-Aug-14	0	
5	165	43	TM	13-Jan-14	0	Riyadh
6			OLI	20-Jan-14	0	
7	166	43	TM	14-Aug-85	0	
8			OLI	16-Aug-14	0	
9	169	45	TM	30-Mar-85	8	Makkah & Al-Taif
10			OLI	4-May-14	3	
11	170	45	TM	9-Jun-85	0	Jeddah
12			OLI	9-Jun-14	0	

3.2. Processing framework

3.2.1. Image classification

The process of urban classification started with image segmentation in eCognition Developer 8.9, which used five scale parameters in Landsat TM images (Fig. 2). However, the segmentation of Landsat OLI images was not executed well enough to determine the land objects (Fig. 3 shows an example of the segmentation performance on Landsat OLI values). In addition, the large data size was difficult to analyze. This was due to differences in the spectral responses and target pixels between the Landsat TM and Landsat OLI images (Li, Jiang, et al., 2013; Flood, 2014). The dynamic range of the Landsat OLI image is 12 bits, while the dynamic range of the Landsat TM is 7. Therefore, the radiance scaling of Landsat OLI can register a digital number (DN) range of $2^{12} = 4096$, which is considerably larger than older Landsat scaling ranges like the more TM common $2^7 = 128$. These large DN values result in approximately one segmentation for each pixel in the image (e.g., a subset of 3000 × 3000 produces more than 6,000,000 objects) (Fig. 3). Processing these objects is time consuming and requires a large computer storage system. To solve this problem, the DN values were converted to Top of Atmosphere (TOA) radiance, using Equation (1) (Chander, Markham, & Helder, 2009) and radiance rescaling factors provided in the header files:

$$L_\lambda = M_L Q_{cal} + A_L \tag{1}$$

where L_λ is the TOA spectral radiance (Watts/(m2 × srad × μm), M_L is the band specific multiplicative rescaling factor, A_L is the band

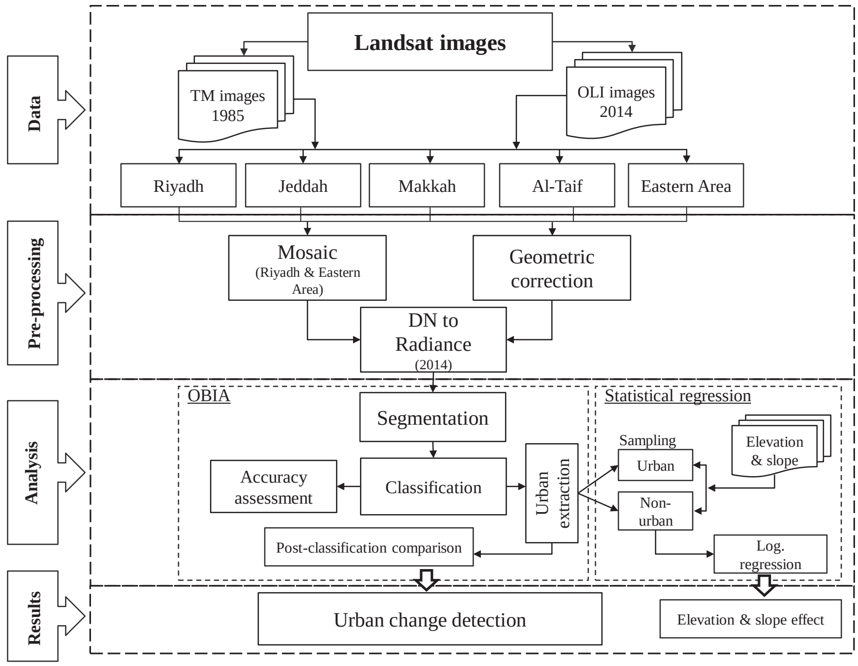

Fig. 2. Flowchart of the classification and statistical processes.

specific additive rescaling factor and Q_{cal} is quantized and calibrated standard product pixel values.

The second step after image segmentation was image classification. All of the images for both sensors were classified separately in the classification scheme. An automated hierarchical classification was applied to the Landsat images using a decision tree structure (Fig. 4). A hierarchical decision tree classifier is an algorithm that labels unknown patterns using a sequence of decisions (Tso and Mather, 2009). The decision tree design is based on a hypothesis (classes), rules (feature sets) and conditions (thresholds). The hypothesis, or classes, determined in this study were water, vegetation, bare soil and urban area (Fig. 4), starting with the classes of significant separability (water and vegetation) and ending with lower separability (bare soil and urban). However, the aim of this study was to detect urban change rather than other land cover features. Thus, only urban change was considered in the results of this study, where an urban area classification implies locations covered by constructed surfaces (Mertes et al., 2014), buildings and impervious surfaces. All open areas, such as green spaces and undeveloped land, were classified as non-urbanized areas.

For automatic classification, feature sets were identified in the

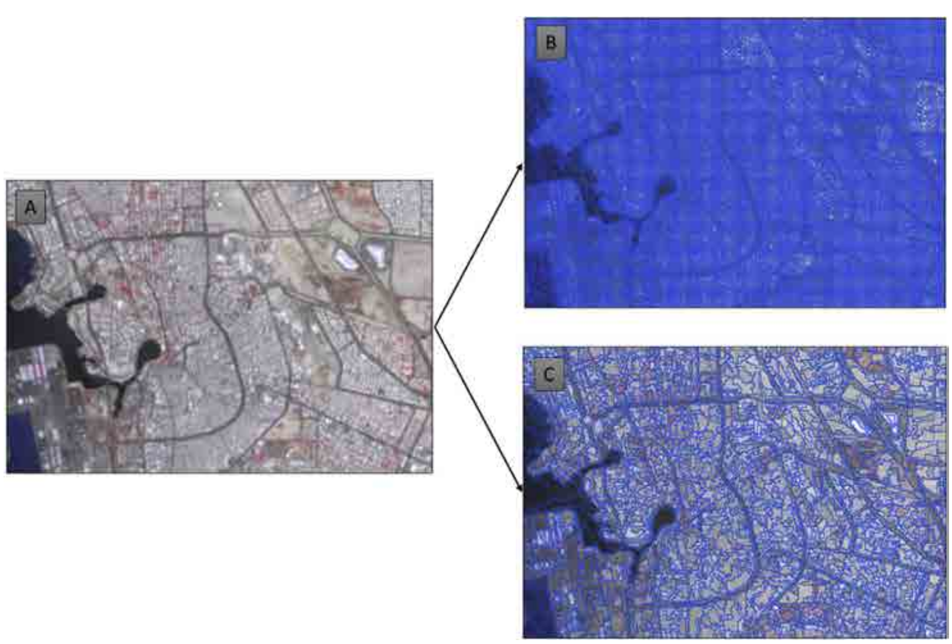

Fig. 3. An example of segmentation analysis of Landsat OLI, A) Landsat OLI image color composition of bands 5, 4 and 3, B) segmentation of DN values and C) segmentation of radiance scale.

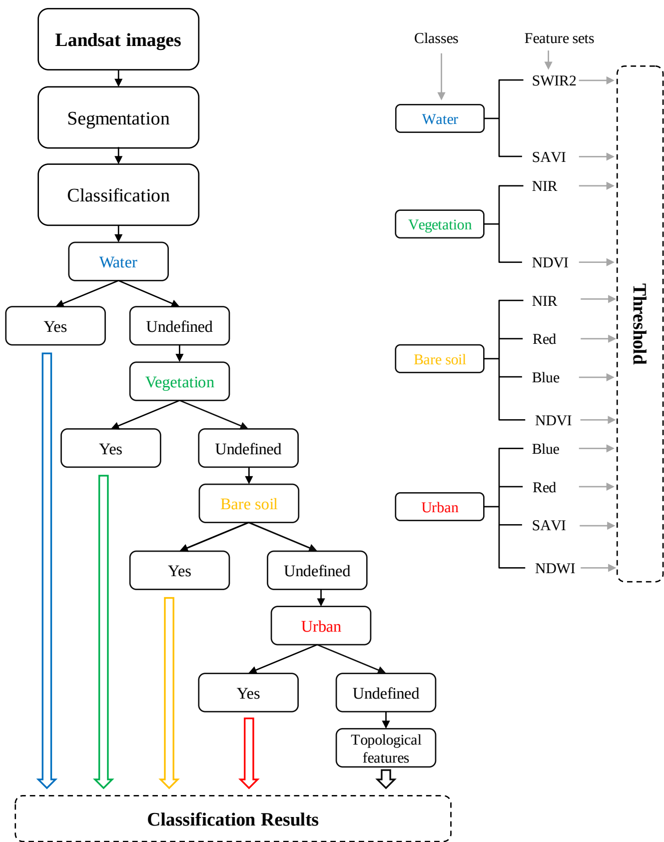

Fig. 4. Decision tree scheme and feature sets used in image classification.

classification platform to effectively distinguish certain categories in the Landsat TM and OLI sensors. Thus, an analysis of the spectral patterns of twelve different features was applied to the Landsat images. Six of these features stemmed from the Landsat TM and OLI sensors, including blue, green, red, near infrared (NIR), short wavelength infrared one (SWIR1) and short wavelength infrared two (SWIR2) bands. In addition, the Normalized Difference Vegetation Index (NDVI) (Rouse, Hass, Schell, & Deering, 1973), as expressed in Equation (2), and Soil Adjusted Vegetation Index (SAVI) (Huete, 1988), as expressed in Equation (3), were applied to existing Landsat bands as proposed by Abelen, Taubenbock, and Stilla (2011) and Taubenböck et al. (2012). The remaining three features were the Normalized Difference Water Index (NDWI) (Gao, 1996; Jackson et al., 2004), as described in Equation (4), and the texture of red and blue bands as extra bands in the existing Landsat TM and OLI bands. Local variance value was conducted to calculate the occurrence texture using a 3 × 3 moving window. However, the textural bands were ignored in the classification analysis due to their limitations in providing accurate results and increasing the size of image segmentation. Thus, only nine features were used to classify the different classes, as described in Fig. 4.

Normalized Difference Vegetation Index (NDVI):

$$NDVI = \frac{DN_{NIR} - DN_{Red}}{DN_{NIR} + DN_{Red}} \tag{2}$$

Soil Adjusted Vegetation Index (SAVI):

$$SAVI = \frac{DN_{NIR} - DN_{Red}}{DN_{NIR} + DN_{Red} + L} \times (1 + L) \tag{3}$$

Normalized Difference Water Index (NDWI):

$$NDWI = \frac{DN_{NIR} - DN_{SWIR1}}{DN_{NIR} + DN_{SWIR1}} \tag{4}$$

3.2.2. Threshold definition

The definition of a threshold is variable and depends on the Landsat scene, user experience and time taken for calibration (Taubenböck et al., 2012). By using the feature sets described above, we adjusted individual thresholds to classify water, vegetation, bare soil and urban areas. Water and vegetation were easily identified by defining the threshold values based on SWIR2 and SAVI features for water and NIR and NDVI features for vegetation. Determining the thresholds for bare soil and urban areas was challenging due to similarities between the spectral responses of these classes. However, by limiting both the threshold values to selected features and the spectral response of a phenomenon, we were able to distinguish between urban areas and bare soil. Moreover, the combining of two thresholds from two features was utilized to extract urban areas and bare soil.

The selected feature sets and threshold values varied from image to image due to differences in the study area characteristics. Therefore, there were no constant feature sets applied to all of the images in this study. We adjusted the feature sets and threshold values for each image and across the 12 images. For example, the spectral response values of the NIR bands were used to extract vegetation cover in all images, while the spectral response values of the same bands were used to extract the sand desert in Riyadh, Jeddah and Eastern Area, which contain large areas of sandy desert. In contrast, for the terrain composition structure, such as that of Makkah and Al-Taif, the NIR band was used only to extract vegetation cover. Therefore, applying threshold values under similar conditions requires consideration when selecting suitable feature sets. Thus, various land cover classes comprising urban extents can be effectively classified. Table 2 shows an example of the feature sets and threshold values selected to classify Riyadh images.

Unclassified segments were analyzed using the relational neighbor objects function, which assumes that the missing classification of an object is related to a neighbor object. Through this process, the classified object that has the greater amount of pixels is used to produce the missing segments. Finally, a manual correction was applied for misclassified objects to modify incorrect classification in all images.

3.2.3. Accuracy assessment

Accuracy assessment determines the quality level of information derived by remote sensing data (Congalton & Green, 2008). The importance of accuracy assessment lies in the link between the remotely sensed data and reference information in order to

Table 2
An example of the threshold values selected for Riyadh.

Class	Feature set	Threshold value
Water	SWIR2	SWIR2 ≤ 25
	SAVI	SAVI ≤ −0.08
Vegetation	NDVI	NDVI ≤ 0.2
	NIR	NIR ≥ 70 and NIR ≤ 110
Bare soil	NIR	NIR > 120
	Blue	Blue > 130 and Blue < 150
	Red	Red > 90
	NDVI	NDVI ≤ 0
Urban	Blue	Blue ≥ 155
	Red	Red ≥ 55 and Red < 80
	SAVI	SAVI ≥ −0.07 and SAVI ≤ −0.05
	NDWI	NDWI ≥ 0.125 and NDWI ≤ 0.25

evaluate the results obtained from satellite data. In this research, the accuracy assessment was conducted using a stratified sampling technique to generate the reference points for all five cities. Land cover classes were selected as strata and had different number of samples based on its distribution. For example, water strata had less random points than vegetation strata in Makkah, Al-Taif and Riyadh while it had a higher number of random samples in coastlines cities such as Jeddah and Eastern Area than vegetation cover class. Google Earth datasets were used to generate the sample points for the 2014 classifications. A total of 500 sample points were selected for the large cities such as Riyadh, Jeddah and Eastern Area and 400 sample points were selected for the other two cities (Makkah and Al-Taif) using multinomial distribution technique (Congalton & Green, 2008). However, in the absence of reference data of 1985, these samples could not be used directly for 1985 accuracy evaluation. Therefore, additional analysis was conducted to make these samples valid to evaluate the accuracy of 1985 classifications. Thus, NDVI differences were computed between 1985 and 2014 and only unchanged pixels from 1985 to 2014 were used to generate samples for 1985 classifications as suggested by Foody (2004 and 2008). After refinement, 310 samples were finalized for Riyadh, Jeddah, and Eastern Area and 260 samples for Makkah and Al-Taif. The accuracy assessment, then, was tested using the traditional method discussed by Congalton, (1991). Producer's accuracy, user's accuracy, overall accuracy and Kappa coefficient were carried out through the use of error matrices individually for each image.

The change detection approach used to identify urban built-up areas in this study was based on a decision tree classification that uses only optical data sets. The population density data of the selected cities were not considered in this analysis. The classification of individual images utilized post-classification comparison for mapping the changes of urban built-up areas between 1985 and 2014. The results of image classification were based on three categories, which are shown in the maps: the urban area of 1985, the urban area of 2014 and water.

3.3. Statistical analysis

A binary logistic regression model has been applied on the selected five cities by Alqurashi, Kumar, and Al-Ghamdi (2016) using four driving force factors including elevation, slope, distance to drainage and distance to major roads. In this study only two variables, including elevation and slope, will be examined to explain the biophysical impact on the current urban growth distribution. The process of statistical analysis was started by creating random sample points that represent urban and non-urban features for each city and were coded as 1 (presence) for urban and 0 (absence) for non-urban features. The sample points were different among cities based on their extent. Thus, a total of 30,000, 20,000 and 25,000 random samples were created for Riyadh, Jeddah and Eastern Area respectively and 10,000 random samples were created for Makkah and Al-Taif for both urban and non-urban features. Then, the logistic regression model was computed on the sample points using the equation presented in Alqurashi et al. (2016). The coefficient values of elevation and slope and the intercept values were used to calculate the relative impact of these variables on urban distribution between 1985 and 2014. More detail about these processes can be found in Alqurashi et al. (2016).

4. Results

4.1. Image classification maps

Figs. 5–9 show the classification results of the urban built-up areas of Riyadh, Jeddah, Makkah, Al-Taif and Eastern Area, respectively. The subset of Riyadh images (Fig. 5) includes the Al-Kharj Governorate, which is approximately 77 km south of the city of Riyadh. From the classification results, it is obvious that all five cities have changed considerably from 1985 to 2014. The distribution of urban areas shows very large and complex urban patterns. Fig. 5 illustrates that the change in urban areas between 1985 and 2014 is distributed from the urban core to the periphery in Riyadh. The urbanized shape is approximately circular, extending from the center towards the margins. In Al-Kharj, a high rate of urbanization has occurred over the last 30 years. The massive urban sprawl in this area can be ascribed to rural urbanization. In contrast, Jeddah (Fig. 6) has a different spatial distribution of urban growth, where the coastline controls the shape of the city. While the city is highly urbanized in the administrative boundary, urban growth is recognized to be distributed north and east, more so than south. The urban growth in Makkah and Al-Taif (Figs. 7 and 8, respectively) is influenced by the topographical structure. However, Makkah has experienced rapid development from the center of the city towards the southern and eastern portions, while the massive growth in Al-Taif is ascribed to rural urbanization. Eastern Area also experienced a high rate of urbanization between 1985 and 2014 (Fig. 9). The rate of urban extent increased in the older portions of the area, as well as experiencing new growth in the southern portion of the area.

The classification results from the Landsat TM and OLI imagery exhibited complex patterns of urban growth across the selected Saudi Arabian cities over the last 30 years. The urban structures are varied in terms of spatial growth, as they are polycentric in Al-Taif and Eastern Area and monocentric in Makkah, Jeddah and Al-Riyadh, excluding Al-Kharj. Thus, the spatial distribution of Al-Taif and Eastern Area exhibits a complex pattern of development, while Makkah, Jeddah and Riyadh are developing from a centroid. While the development of monocentric cities allows a double structure, the polycentric cities have a complex development. Therefore, the varied results from the urban spatial distributions across the five cities suggest significant complexity and heterogeneous urban development.

4.2. Urban measurement

The spatiotemporal measurement of urban growth is an important analysis. The quantification of the urban extent of the five cities areas was calculated in hectares. Table 3 shows the comparison of the statistical information from urban areas in 1985 and 2014. The amount of development has increased in all five cities over the time period analyzed. However, we observed that Al-Taif, Jeddah, and Eastern Area have developed more than others during the period between 1985 and 2014 with percentages of 184, 165, and 136 respectively. Makkah exhibited the lowest growth among the five cities by approximately 89%, but still experienced massive development. The urban extent in the city of Riyadh measured 55,410 ha in 1985 and expanded to 112,144 ha in 2014. The urban growth of Eastern Area shows an enormous difference between 1985 and 2014 (42,478 in 1985–100,097 in 2014). The urban extent in Jeddah showed a large change as well, from 23,323 ha in 1985–61,720 ha in 2014. Thus, the quantification of urban extent showed high growth in all five cities over the time period studied.

4.3. Accuracy assessment

An accuracy assessment is important for evaluating the information that is provided by satellite image classification. By following the method discussed by Congalton, (1991), Table 4 lists the accuracy assessment of results produced in this study, including

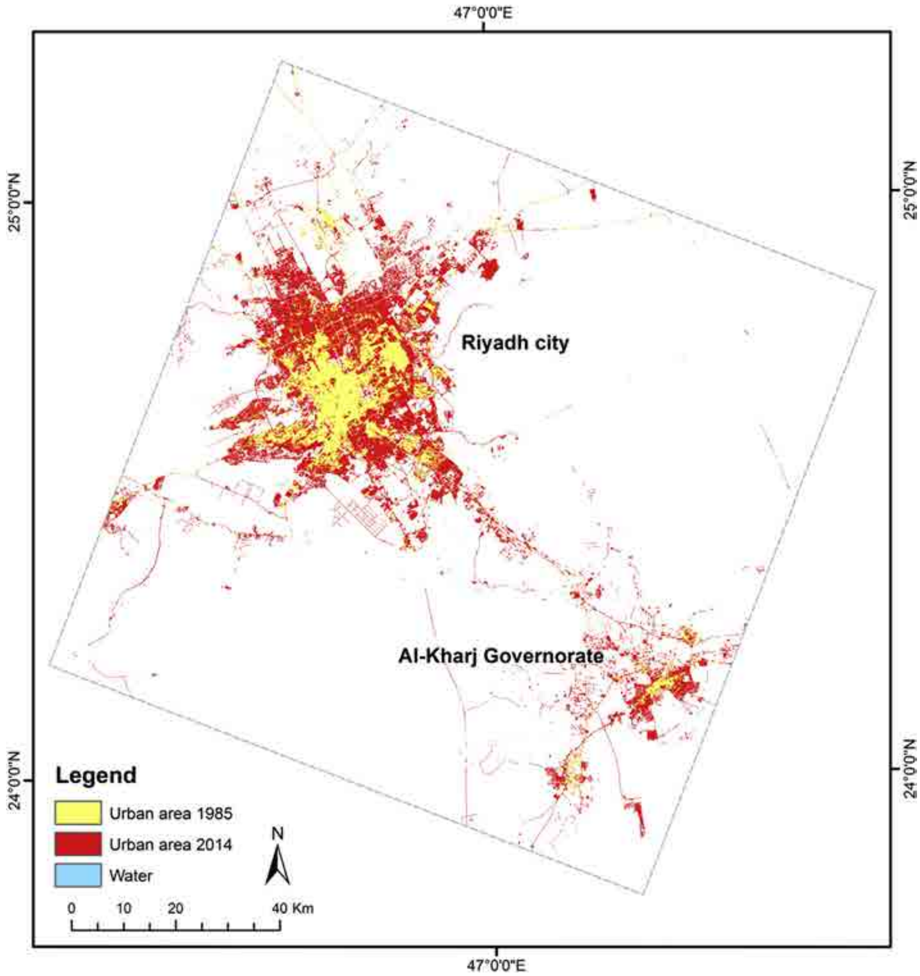

Fig. 5. Urban change in Riyadh.

the producer's and user's accuracies, overall accuracy and Kappa coefficient. The urban change classification resulted in high and consistent accuracy values in the five cities. The overall accuracies ranged from 86% to 93%, which is considered to be satisfactory. Both producer's and user's accuracies provided higher values. However, user's accuracies showed a slightly higher percentage than producer's accuracies. Although both Landsat sensors achieved good overall accuracies and Kappa coefficients, the Landsat OLI provided a slight improvement over the Landsat TM in both the overall accuracy and Kappa coefficient.

4.4. *Spatial effect of elevation and slope on urban distribution*

Fig. 10 shows the spatial effect of elevation and slope variables on the urban distribution in A) Riyadh, B) Jeddah, C) Makkah, D) Al-Taif, and E) Eastern Area between 1985 and 2014. As shown in the figure, elevation and slope clearly controlled the distribution of urban growth between 1985 and 2014 in almost all five cities. However, Eastern Area was the least affected city while Makkah and Al-Taif were the most affected cities by both elevation and slope factors. For Jeddah, the elevated areas in the eastern part of the city clearly controlled the growth and will likely continue to affect the future development in this part of the city. Similarly for Riyadh, the relatively steep slopes in the south-east of the city obviously controlled the distribution of urban growth in the city between 1985 and 2014 and will likely affect the future growth.

Table 5 lists the statistical results of the logistic regression model of elevation and slope variables in the five cities. Slope was statistically significant at $\alpha = 0.001$ level in Riyadh, Makkah and Al-Taif while it showed insignificance in Jeddah and Eastern Area. Elevation, in contrast, was statistically significant in Jeddah at $\alpha = 0.001$ level and $\alpha = 0.01$ level in Riyadh and insignificant in Makkah, Al-Taif and Eastern Area. Both slope and elevation showed insignificance in Eastern Area.

5. Discussion

The results presented in this study show a high rate of urbanization from 1985 to 2014 across the five Saudi Arabian cites studied: Riyadh, Jeddah, Makkah, Al-Taif and Eastern Area. Similar to results reported by Dewan and Yamaguchi, (2009), who found that the built-up area in Dhaka, Bangladesh increased by approximately 190% from 1975 to 2003. The urban expansion in the selected cities was influenced by two factors, including the government policy during the development process and increases in migration towards the five cities. These two factors mainly resulted from the development of the country's economy, which is heavily dependent on oil revenues. Increasing oil prices over the past 30 years have significantly contributed to increases in the urban growth of the five cities. Urban and economic growth in these cities has significantly impacted a number of environmental components as well as contributed to a decrease in natural resources during the study

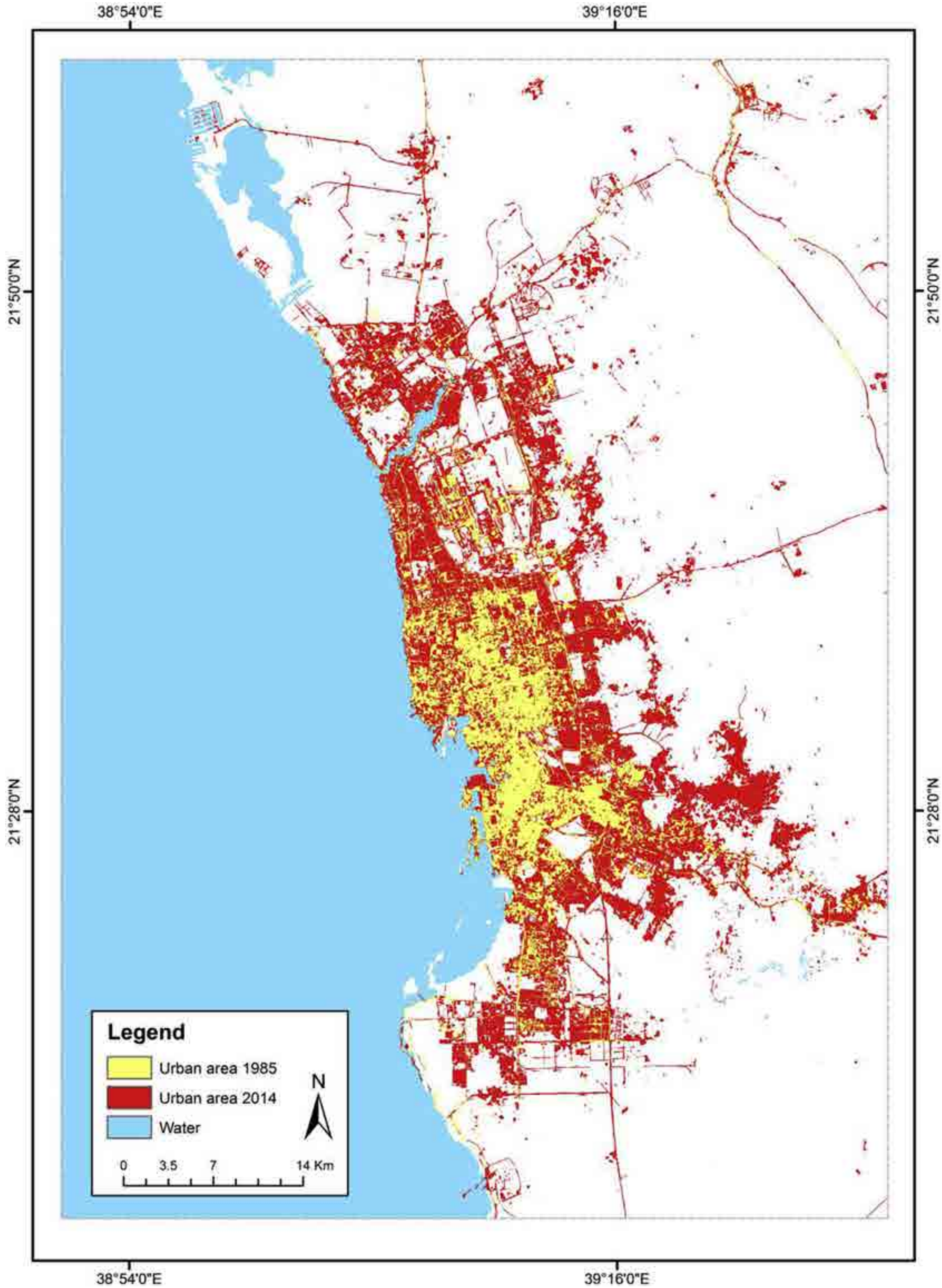

Fig. 6. Urban change in Jeddah.

period.

The development process in Saudi Arabia has slowed since the mid-1980s and the Gulf War in the early 1990s (Al-Butʹhie and Eben Saleh, 2002). However, from 1990 through June 2014, oil prices increased significantly (e.g. from US $35.5 per barrel in 1980 to around US $109 in 2012) (OPEC, 2015), which allowed for increases in the national budgets of the country. The massive budgets (e.g., up to US $296 billion in 2011) have been used to extensively support the development process across the country (Ministry of Finance, 2011). The government support is based on providing interest-free loans to both public and private sectors and establishing industrial cities across the county through master plans.

The construction of housing is largely funded through the advance of no-interest loans by the government to support the development process and to decrease the housing shortage (Al-Hathloul & Mughal, 2004; Gamboa, 2008). Moreover, the

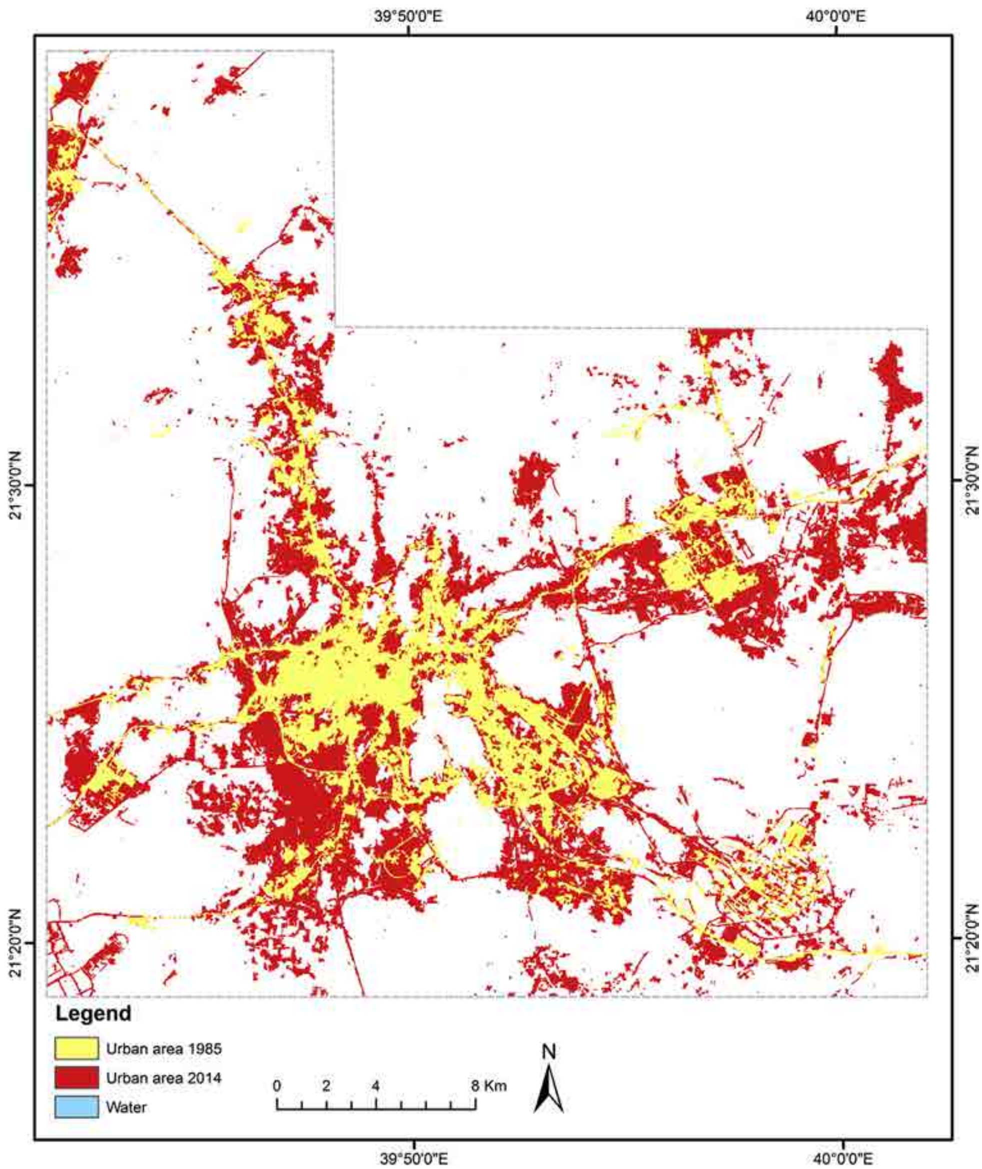

Fig. 7. Urban change in Makkah.

government has established five specialized credit institutions to provide investment loans for citizens to support the private sector and to increase job opportunities (Alshahrani & Alsadiq, 2014). Providing no-interest loans and free land-plot grants for low-income nationals has led to a significant urban expansion over a short period of time.

Although government support has significantly contributed to the increase in urban sprawl across the country, the socioeconomic benefits of the five cities are attractive to people who are seeking a better job or life. The different characteristics of each city have led to increases in both internal and external migration, which has largely expanded the cities. For example, the growth of the tourism sector over the last 30 years has converted Al-Taif from a small town, settled by farmers in the center and tribes on the margins, to a modern city and a major tourism center in Saudi Arabia. Moreover, the oil industry development in Eastern Area, commercial advantages in Jeddah, job demand in the government sector in Riyadh and religious circumstances in Makkah have significantly contributed to increasing urban cover in these cities.

Urbanization is a human activity that is recognized as a key element that affects various environmental components and natural resources (Alberti & Marzluff, 2004). It contributes to increases in carbon dioxide (CO_2) and other pollutant emissions (Dhakal, 2009; Glaeser & Kahn, 2010; Ma, Liu, & Chai, 2015). Naturally, the physical environment in Saudi Arabia has experienced a number of negative environmental impacts, such as increased temperatures, the unavailability of water, soil erosion and other factors, which pose a serious environmental threat. This threat is enhanced due to the extreme climate and desert environments. The impact of human activities occurs at a faster rate than natural influences. The main environmental issue in Saudi Arabia relates to the locations of residential and industrial activities, which are often situated near sensitive environmental areas, such as coastal zones, mountains and unique desert habitats (Vincent, 2008). Such activities have damaged these sensitive environments in some locations. In terms of coastal and land biodiversity, the increase of urbanization and industrial activities in the five cities has decreased biotic ecosystems. In Saudi Arabia, the main problem confronting biodiversity is

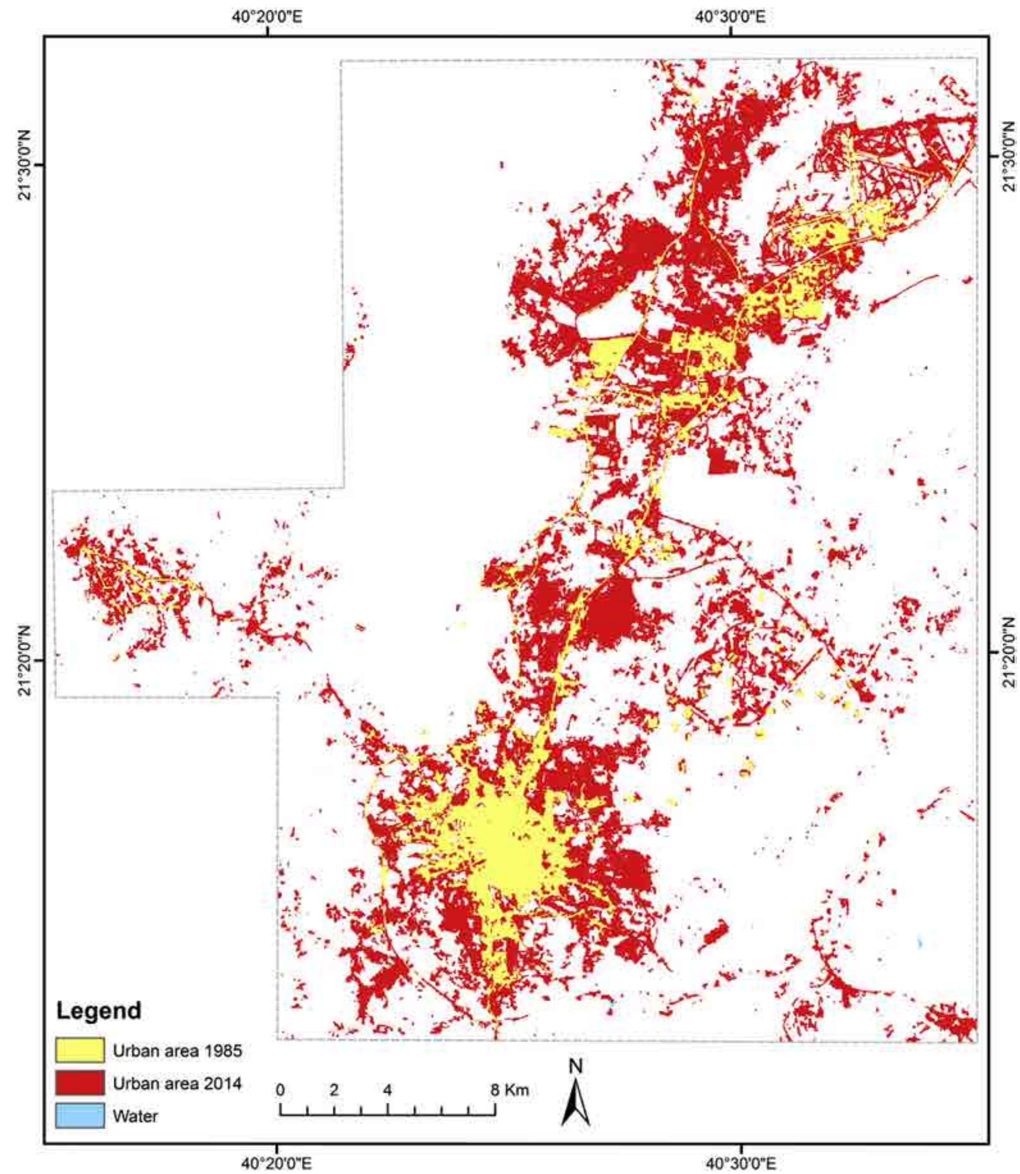

Fig. 8. Urban change in Al-Taif.

environmental pollution, which results from economic and urban growth (Alzahrani & Alqasmi, 2013). The extreme economic diversification policy, which is based on expanding manufacturing and heavy industries and increased urban growth, has led to a significant degradation to the natural components of Saudi Arabia over the last 30 years.

Air pollution is becoming a concern in the fast growing cities in Saudi Arabia. The growing transportation and industrial sectors emit a number of harmful gases, including CO_2, nitrogen dioxide (NO_2), sulfur dioxide (SO_2) and volatile organic compounds (Husain & Khalil, 2013, p. p14). The most emitted gas in the Saudi Arabian cities is CO_2. According to the Center for Global Development, Saudi Arabia was among the top 30 countries in the world with the highest CO_2 emissions in 2007, with approximately 57,9000,000 tons of emissions (Tolba & Saab, 2008). The CO_2 emission rate has increased more rapidly than other gases in recent years due to the increase in industrial and urban activities. The expansion of the transportation systems and residential areas, increases in oil production (e.g., from 41 million barrels in 1980 to over 245 million barrels in 2010) and industrial activities combine to produce the majority of the CO_2 emissions in the five cities. The power and electricity sector is the top contributor to CO_2 emissions (Taher & Al-Hajjar, 2013). Jeddah is the most polluted city in Saudi Arabia (Vincent, 2008). The industrial parts of the city, the area south of the city and regions beyond the urban area contribute significant amounts of airborne pollution. In addition, the King Abdulaziz International Airport, in the north, and the desalinization plant, in the west, are located near residential areas, as well as other facilities, including hospitals and schools (Vincent, 2008). The industrial sector in Eastern Area and the complex transportation system in Riyadh also contribute large amounts of gases. While the relevant sectors in Saudi Arabia are currently not able to provide precise information on the health effects, the emissions of these elements are largely recognized as harmful worldwide.

The massive urban cover expansion in the five selected cities has been uncontrolled and has created numerous problems. The different government sectors mainly contributed to the creation of these problems. A major issue is the absence of coordination

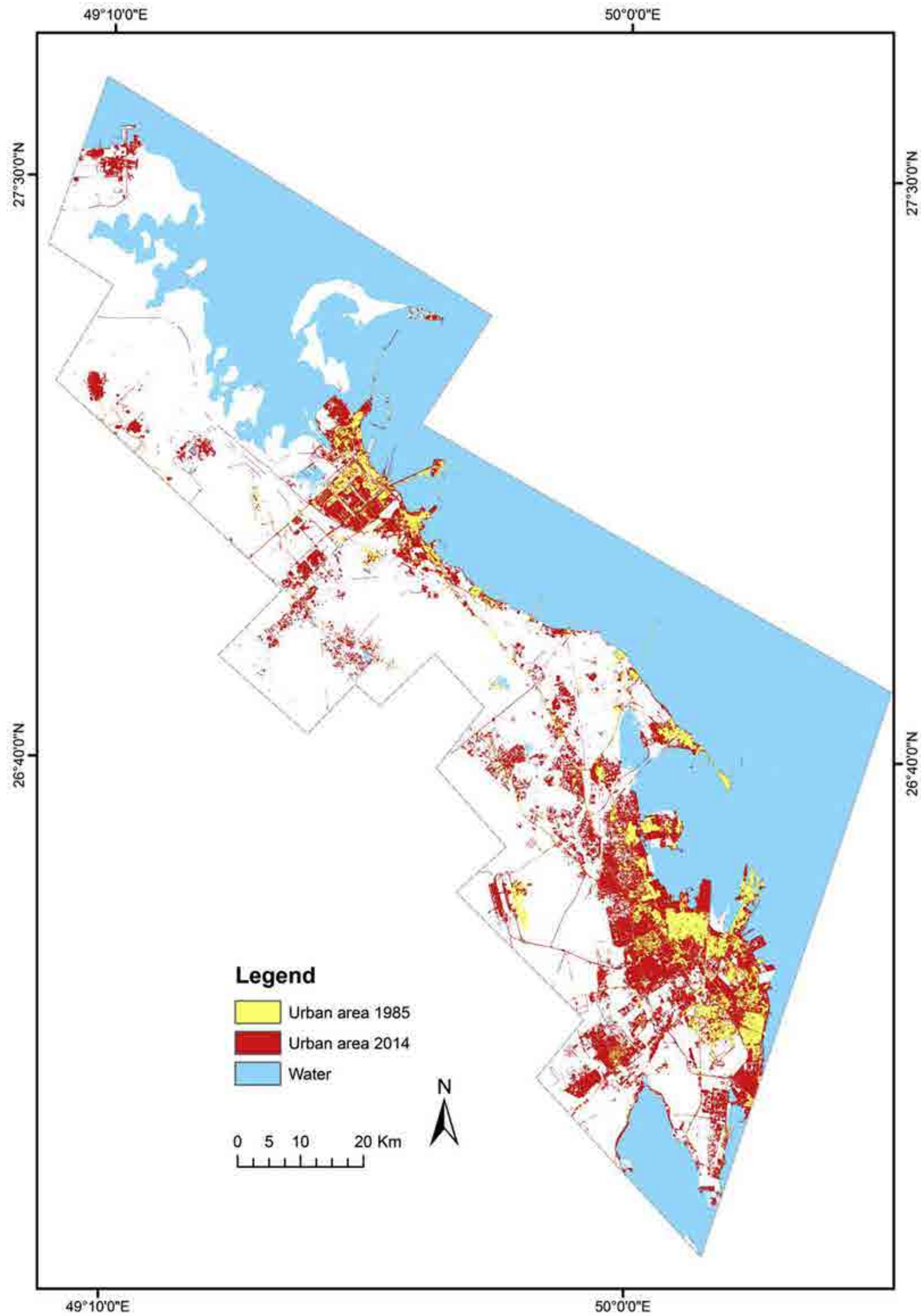

Fig. 9. Urban change in Eastern Area.

between sectors during the development process. For example, the public services that manage road construction rarely communicate with the residential construction sector, which has resulted in complex transportation problems. Another factor related to economic growth is that in Saudi Arabia, the desire for multifaceted economic diversification is a major priority and economic interests often override environmental concerns (Alzahrani & Alqasmi, 2013). Furthermore, there is a lack of consideration of the environmental and health impacts resulting from urban expansion from both decision makers and implementers in the five cities.

Although there is an effort from different organizations, including the government sectors, to assess and manage the environment and natural resource in the five cities, Saudi Arabia is still far from a successful implementation of sustainable development strategies and commitment from the relevant authorities. Also, the public participation is limited in the environmental impact

Table 3
Statistical information of urban growth between 1985 and 2014.

City	Area (ha)		Difference	Increase (%)
	1985	2014	2014–1985	
Riyadh	55,410	112,144	56,734	102
Jeddah	23,323	61,720	38,397	165
Makkah	12,658	23,887	11,229	89
Al-Taif	6311	17,950	11,639	184
Eastern Area	42,478	100,097	57,619	136

Table 4
Accuracy assessment of urban change classification.

City	Landsat TM (1985)				Landsat OLI (2014)			
	Producer's accuracy	User's accuracy	Overall accuracy	Kappa coefficient	Producer's accuracy	User's accuracy	Overall accuracy	Kappa coefficient
Riyadh	73.58	88.31	90.27	0.76	83.5	92.71	93.79	0.86
Jeddah	78.01	79.75	89.77	0.84	81.26	85.17	90.89	0.87
Makkah	76.82	89.71	89.05	0.79	88.61	94.22	91.86	0.85
Al-Taif	75.95	85.13	86.74	0.74	89.57	79.61	88.37	0.80
Eastern Area	73.46	87.93	89.91	0.86	86.18	89.51	89.31	0.83

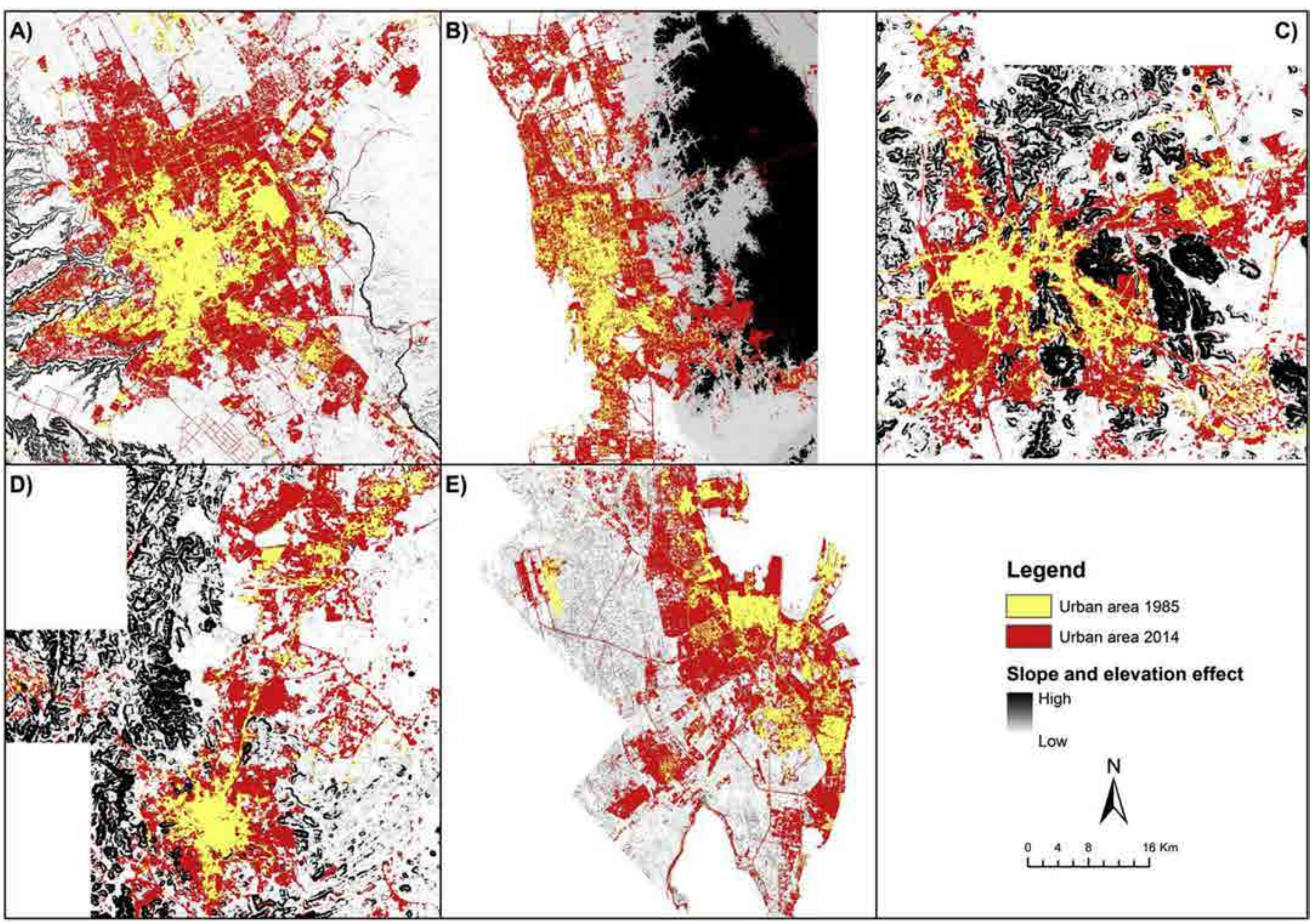

Fig. 10. The effect of elevation and slope variables on urban distribution in A) Riyadh, B) Jeddah, C) Makkah, D) Al-Taif, E) Eastern Area.

assessment plan. More effort is necessary and only possible by emphasizing coordination between the involved sectors, as well as binding legislation related to environmental conservation.

Given the abilities of optical remote sensing data, the information associated with spatiotemporal distributions, and natural processes, changes can be effectively investigated for two or more intervals. This work has shown the advantage of using multi-temporal satellite images to measure and quantify the spatial

Table 5
The statistical results of logistic regression model of elevation and slope.

Variable	Coefficient	Std. Error	z value	P (>|z|)
Riyadh				
Intercept	−0.2036754	0.247018	−0.825	0.4096
Elevation	0.000899*	0.000411	2.187	0.0288
Slope	−0.0502531***	0.006318	−7.954	1.80E-15
Jeddah				
Intercept	1.055623***	0.067906	15.545	<2e-16
Elevation	−0.019591***	0.001179	−16.62	<2e-16
Slope	−0.008453	0.007843	−1.078	0.281
Makkah				
Intercept	0.7342276**	0.237581	3.09	0.002
Elevation	−0.0005003	0.000767	−0.652	0.514
Slope	−0.0584739***	0.006955	−8.407	<2e-16
Al-Taif				
Intercept	−0.2240267	0.6733	−0.333	0.739
Elevation	0.0005582	0.000435	1.284	0.199
Slope	−0.1046852***	0.010097	−10.368	<2e-16
Eastern Area				
Intercept	−0.053161	0.0852	−0.624	0.533
Elevation	0.003483	0.004693	0.742	0.458
Slope	−0.023528	0.015336	−1.534	0.125

Significant code: ***$P < 0.001$, **$P < 0.01$.

growth over a time period in five selected cities. Moreover, the nature and complexity of the urban change patterns have been identified. The accurate monitoring of urban footprints over time can help to assess and evaluate the urbanization process.

6. Conclusion and summary

The results of this study indicate a high rate of urbanization in Saudi Arabian cites between 1985 and 2014. All five cities included in this research, Riyadh, Jeddah, Makkah, Al-Taif and Eastern Area, experienced very large developments over the last 30 years. The spatiotemporal pattern analysis indicates that the urbanization process in the selected five cities was both complex and dynamic. This is due to an increase in the country's economy, which is heavily oil dependent. Increased oil prices have led to the expansion of the Saudi Arabian cities over the past 30 years, particularly since the government has emphasized large-scale development. The results from the analysis demonstrate that if future development continues at the same rate, negative environmental impacts associated with urban growth are likely to occur. Sustainable development must be included for further urbanization.

This research used only remote sensing data to detect urban expansion between 1985 and 2014. Moreover, the role of government policy and the increase of oil prices were linked and included as they have significantly influenced the urban growth in the five selected cities in Saudi Arabia. In addition, the effects of two biophysical variables (elevation and slope) on the spatial distribution of urban growth between 1985 and 2014 in the five cities were examined and presented in the study. However, analysis of various socioeconomic factors and population growth are not included because of data limitations over the time period of the study. Including such factors may provide more refinement of the urban growth process in the Saudi Arabian cities. Nevertheless, the results presented in this research provide the essential information of the spatiotemporal changes in the past to support the local authorities and the decision-making processes in these cities for further developments.

References

Abelen, S., Taubenbock, H., & Stilla, U. (2011). *Interactive classification of urban areas using decision trees*. Paper read at Urban Remote Sensing Event (JURSE), 2011 Joint, at Munich, Germany.

Al-Buťhie, I. M., & Eben Saleh, M. A. (2002). Urban and industrial development planning as an approach for Saudi Arabia: The case study of Jubail and Yanbu. *Habitat International, 26*(1), 1–20. http://dx.doi.org/10.1016/S0197-3975(01)00026-1.

Al-Ghamdi, S., & Al-Naggar, Y. (2002). Analyzing the urban growth and its directions using remote sensing data: An applied study for Makkah city between 1978 and 2000 (in Arabic). *Journal of King Abdel-Aziz University*, 231–272. A special issue.

Al-Ghamdi, K., Mirza, M., Elzahrany, R., & Dawod, G. (2012). *GIS evaluation of urban growth and flood hazards: A case study of Makkah city, Saudi Arabia*. Presented at the FIG working week, Rome, Italy, May 6–10.

Al-Hathloul, S., & Mughal, M. A. (2004). Urban growth management-the Saudi experience. *Habitat International, 28*(4), 609–623.

Alberti, M. (2005). The effects of urban patterns on ecosystem function. *International Regional Science Review, 28*(2), 168–192.

Alberti, M., & Marzluff, J. (2004). Ecological resilience in urban ecosystems: Linking urban patterns to human and ecological functions. *Urban Ecosystems, 7*(3), 241–265. http://dx.doi.org/10.1023/B: UECO.0000044038.90173.c6.

Aljoufie, M. (2014). Spatial analysis of the potential demand for public transport in the city of Jeddah, Saudi Arabia. *Urban Transport XX, 138*, 113.

Aljoufie, M., Zuidgeest, M., Brussel, M., & van Maarseveen, M. (2013). Spatial–temporal analysis of urban growth and transportation in Jeddah City, Saudi Arabia. *Cities, 31*(0), 57–68. http://dx.doi.org/10.1016/j.cities.2012.04.008.

Alqurashi, A., & Kumar, L. (2014). Land use and land cover change detection in the Saudi Arabian desert cities of Makkah and Al-Taif using satellite data. *Advances in Remote Sensing, 3*, 106–119. http://dx.doi.org/10.4236/ars.2014.33009.

Alqurashi, A. F., Kumar, L., & Al-Ghamdi, K. A. (2016). Spatiotemporal modeling of urban growth predictions based on driving force factors in five Saudi Arabian cities. *ISPRS International Journal of Geo-Information, 5*(8), 139. http://www.mdpi.com/2220-9964/5/8/139.

Alshahrani, S., & Alsadiq, A. (2014). *Economic growth and government spending in Saudi Arabia: An empirical investigation*. International Monetary Fund.

Alzahrani, D., & Alqasmi, H. (2013). Protecting the biodiversity of the Arabic Gulf's coastal waters from agricultural and industrial runoff case Study-Saudi Arabia. *International Journal of Social Science and Humanity, 3*(1). 62-n/a http://dx.doi.org/10.7763/IJSSH.2013.V3.195.

Bagan, H., & Yamagata, Y. (2012). Landsat analysis of urban growth: How Tokyo became the world's largest megacity during the last 40 years. *Remote Sensing of Environment, 127*(0), 210–222. http://dx.doi.org/10.1016/j.rse.2012.09.011.

Bobylev, N. (2009). Mainstreaming sustainable development into a city's master plan: A case of urban underground space use. *Land Use Policy, 26*(4), 1128–1137. http://dx.doi.org/10.1016/j.landusepol.2009.02.003.

Chander, G., Markham, B. L., & Helder, D. L. (2009). Summary of current radiometric calibration coefficients for Landsat MSS, TM, ETM+, and EO-1 ALI sensors. *Remote Sensing of Environment, 113*(5), 893–903. http://dx.doi.org/10.1016/j.rse.2009.01.007.

Congalton, R. G. (1991). A review of assessing the accuracy of classifications of remotely sensed data. *Remote Sensing of Environment, 37*(1), 35–46.

Congalton, R. G., & Green, K. (2008). *Assessing the accuracy of remotely sensed data: Principles and practices*. CRC press.

Dewan, A. M., & Yamaguchi, Y. (2009). Land use and land cover change in greater Dhaka, Bangladesh: Using remote sensing to promote sustainable urbanization. *Applied Geography, 29*(3), 390–401.

Dhakal, S. (2009). Urban energy use and carbon emissions from cities in China and policy implications. *Energy Policy, 37*(11), 4208–4219. http://dx.doi.org/10.1016/j.enpol.2009.05.020.

Flood, N. (2014). Continuity of reflectance data between Landsat-7 ETM+ and Landsat-8 OLI, for both top-of-atmosphere and surface reflectance: A study in the Australian landscape. *Remote Sensing, 6*(9), 7952–7970.

Foody, G. M. (2004). Thematic map comparison: Evaluating the statistical significance of differences in classification accuracy. *Photogrammetric Engineering & Remote Sensing, 70*(5), 627–633.

Foody, G. M. (2008). Harshness in image classification accuracy assessment. *International Journal of Remote Sensing, 29*(11), 3137–3158. http://dx.doi.org/10.1080/01431160701442120.

Fulton, W. B., Pendall, R., Nguyen, M., & Harrison, A. (2001). *Who sprawls most?: How growth patterns differ across the US*. Washington, DC: Brookings Institution, Center on Urban and Metropolitan Policy.

Gamboa, J. (2008). City Expanding to the Desert Horizon: Riyadh's problem of explosive growth and urban sprawl. *Geography*, 554.

Gao, B. (1996). NDWI—a normalized difference water index for remote sensing of vegetation liquid water from space. *Remote Sensing of Environment, 58*(3), 257–266.

Giri, C. P. (2012). *Remote sensing of land use and land Cover: Principles and applications*. CRC Press.

Glaeser, E. L., & Kahn, M. E. (2010). The greenness of cities: Carbon dioxide emissions and urban development. *Journal of Urban Economics, 67*(3), 404–418. http://dx.doi.org/10.1016/j.jue.2009.11.006.

Grimmond, S. (2007). Urbanization and global environmental change: Local effects of urban warming. *The Geographical Journal, 173*(1), 83–88.

Huete, A. R. (1988). A soil-adjusted vegetation index (SAVI). *Remote Sensing of Environment, 25*(3), 295–309. http://dx.doi.org/10.1016/0034-4257(88)90106-X.

Husain, T., & Khalil, A. A. (2013). Environment and sustainable development in the kingdom of Saudi Arabia: Current status and future strategy. *Journal of*

Sustainable Development, 6(12), p14.

Jackson, T. J., Chen, D., Cosh, M., Li, F., Anderson, M., Walthall, C., et al. (2004). Vegetation water content mapping using Landsat data derived normalized difference water index for corn and soybeans. *Remote Sensing of Environment, 92*(4), 475–482.

Jat, M. K., Garg, P. K., & Khare, D. (2008). Modelling of urban growth using spatial analysis techniques: A case study of Ajmer city (India). *International Journal of Remote Sensing, 29*(2), 543–567.

Jia, T., & Jiang, B. (2010). *Measuring urban sprawl based on massive street nodes and the novel concept of natural cities*. arXiv preprint arXiv:1010.0541.

Li, P., Jiang, L., & Feng, Z. (2013). Cross-comparison of vegetation indices derived from Landsat-7 enhanced thematic mapper plus (ETM+) and Landsat-8 operational land imager (OLI) sensors. *Remote Sensing, 6*(1), 310–329.

Li, X., Zhou, W., & Ouyang, Z. (2013). Forty years of urban expansion in Beijing: What is the relative importance of physical, socioeconomic, and neighborhood factors? *Applied Geography, 38*(0), 1–10. http://dx.doi.org/10.1016/j.apgeog.2012.11.004.

Lu, D., Hetrick, S., Moran, E., & Li, G. (2010). Detection of urban expansion in an urban-rural landscape with multitemporal QuickBird images. *Journal of Applied Remote Sensing, 4*(1), 041880–041880-17.

Ma, J., Liu, Z., & Chai, Y. (2015). The impact of urban form on CO_2 emission from work and non-work trips: The case of Beijing, China. *Habitat International, 47*, 1–10. http://dx.doi.org/10.1016/j.habitatint.2014.12.007.

Martin, H. (2009). Some recommendations for global efforts in urban monitoring and assessments from remote sensing. In *Global mapping of human settlement*. CRC Press.

Masek, J. G., Lindsay, F. E., & Goward, S. N. (2000). Dynamics of urban growth in the Washington DC metropolitan area, 1973-1996, from Landsat observations. *International Journal of Remote Sensing, 21*(18), 3473–3486.

Mertes, C. M., Schneider, A., Sulla-Menashe, D., Tatem, A. J., & Tan, B. (2014). Detecting change in urban areas at continental scales with MODIS data. *Remote Sensing of Environment*, (0). http://dx.doi.org/10.1016/j.rse.2014.09.023.

Ministry of Finance. (2011). *Ministry of finance press release. Recent economic developments and highlights of fiscal years 2010 and 2011* (Vol. 07). Riyadh, Saudi Arabia: Ministry of Finance. Avaliable from http://www.mof.gov.sa/english/DownloadsCenter/Pages/Budget.aspx.

Mubarak, F. A. (2004). Urban growth boundary policy and residential suburbanization: Riyadh, Saudi Arabia. *Habitat international, 28*(4), 567–591.

OPEC. (2015). *Monthly oil market report*. Vienna, Austria: OPEC Organization.

Pendall, R. (1999). Do land-use controls cause sprawl? *Environment and Planning B: Planning and Design, 26*(4), 555–571.

Rahman, M. (2016). Detection of land use/land cover changes and urban sprawl in Al-Khobar, Saudi Arabia: An analysis of multi-temporal remote sensing data. *ISPRS International Journal of Geo-Information, 5*(2), 15. http://www.mdpi.com/2220-9964/5/2/15.

Rahman, A., Aggarwal, S. P., Netzband, M., & Fazal, S. (2011). Monitoring urban sprawl using remote sensing and GIS techniques of a fast growing urban centre, India. *Selected Topics in Applied Earth Observations and Remote Sensing, IEEE Journal of, 4*(1), 56–64.

Ramankutty, N., & Foley, J. A. (1998). Characterizing patterns of global land use: An analysis of global croplands data. *Global Biogeochemical Cycles, 12*(4), 667–685.

Reilly, M. K., O'Mara, M. P., & Seto, K. C. (2009). From Bangalore to the Bay Area: Comparing transportation and activity accessibility as drivers of urban growth. *Landscape and Urban Planning, 92*(1), 24–33. http://dx.doi.org/10.1016/j.landurbplan.2009.02.001.

Rouse, J. W., Hass, R. H., Schell, J. A., & Deering, D. W. (1973). Monitoring vegetation systems in the great plains with ERTS. In Stanley C. Freden, Enrico P. Mercanti, & Margaret A. Becker (Eds.), *Third ERTS symposium*. Washington, D.C: NASA.

Schneider, A., Friedl, M. A., & Potere, D. (2010). Mapping global urban areas using MODIS 500-m data: New methods and datasets based on 'urban ecoregions'. *Remote Sensing of Environment, 114*(8), 1733–1746. http://dx.doi.org/10.1016/j.rse.2010.03.003.

Seto, K. C. (2009). Global urban issues: A primer. In P. Gamba, & M. Herold (Eds.), *Global mapping of human settlements: Experiences, data sets, and prospects*.

Small, C. (2003). High spatial resolution spectral mixture analysis of urban reflectance. *Remote Sensing of Environment, 88*(1–2), 170–186. http://dx.doi.org/10.1016/j.rse.2003.04.008.

Sugg, Z. P., Finke, T., Goodrich, D. C., Moran, M. S., & Yool, S. R. (2014). Mapping impervious surfaces using object-oriented classification in a semiarid urban region. *Photogrammetric Engineering & Remote Sensing, 80*(4), 343–352. http://dx.doi.org/10.14358/PERS.80.4.343.

Taher, N., & Al-Hajjar, B. (2013). *Energy and environment in Saudi Arabia: Concerns & opportunities*. Springer Science & Business Media.

Taubenböck, H., Esch, T., Felbier, A., Wiesner, M., Roth, A., & Dech, S. (2012). Monitoring urbanization in mega cities from space. *Remote Sensing of Environment, 117*(0), 162–176. http://dx.doi.org/10.1016/j.rse.2011.09.015.

Taubenböck, H., Esch, T., Wiesner, M., Felbier, A., Marconcini, M., Roth, A., et al. (2014). Spatial Dynamics and Patterns of Urbanization: The Example of Chinese Megacities Using Multitemporal EO Data. In *Global urban monitoring and assessment through earth observation* (pp. 171–194). CRC Press.

Taubenböck, H., Wiesner, M., Felbier, A., Marconcini, M., Esch, T., & Dech, S. (2014). New dimensions of urban landscapes: The spatio-temporal evolution from a polynuclei area to a mega-region based on remote sensing data. *Applied Geography, 47*, 137–153.

Tolba, M., & Saab, N. (2008). In Mostafa Tolba, & Najib Saab Beriut (Eds.), *Arab environment future challenges*. Lebanon: The Arab Forum fo Environment and Development.

Tso, B., & Mather, P. (2009). *Classification methods for remotely sensed data* (2nd ed.). CRC press, 376 p.

Torrens, Paul M. (2008). A toolkit for measuring sprawl. *Applied Spatial Analysis and Policy, 1*(1), 5–36.

Vincent, P. (2008). *Saudi Arabia: An environmental overview*. CRC Press.

Vitousek, P. M., Mooney, H. A., Lubchenco, J., & Melillo, J. M. (1997). Human domination of Earth's ecosystems. *Science, 277*(5325), 494–499.

Weng, Q. (2014). What is special about global urban remote sensing?. In *Global urban monitoring and assessment through earth observation*. CRC Press.

Wentz, E. A., Nelson, D., Rahman, A., Stefanov, W. L., & Roy, S. S. (2008). Expert system classification of urban land use/cover for Delhi, India. *International Journal of Remote Sensing, 29*(15), 4405–4427.